A simulation experiment for optimal design hyetograph selection

Lorenzo Alfieri,* Francesco Laio and Pierluigi Claps

Dipartimento di Idraulica, Trasporti ed Infrastrutture Civili, Politecnico di Torino, Corso Duca degli Abruzzi 24, 10129 Turin, Italy

Abstract:

The aim of this work is to assess the accuracy of literature design hyetographs for the evaluation of peak discharges during flood events. Five design hyetographs are examined in a set of simulations, based upon the following steps: (i) an ideal river basin is defined, characterized by a Beta distribution shaped unit hydrograph (UH); (ii) 1000 years of synthetic rainfall are artificially generated; (iii) a discharge time-series is obtained from the convolution of the rainfall time-series and the UH, and the reference T-years flood is computed from this series; (iv) for the same return period T, the parameters of the intensity–duration–frequency (IDF) curve are estimated from the 1000 years of synthetic rainfall; (v) five design hyetographs are determined from the IDF curves and are convolved with the discrete UH to find the corresponding design hydrographs; (vi) the hydrograph peaks are compared with the reference T-years flood and the advantages and drawbacks of each of the five approaches are evaluated. The rainfall and UH parameters are varied, and the whole procedure is repeated to assess the sensitivity of results to the system configuration.

We found that all design hyetographs produce flood peak estimates that are consistently biased in most of the climatic and hydrologic conditions considered. In particular, significant underestimation of the design flood results from the adoption of any rectangular hyetograph used in the context of the rational formula. In contrast, the Chicago hyetograph tends to overestimate peak flows. In two cases it is sufficient to multiply the result by a constant scaling factor to obtain robust and nearly unbiased estimates of the design floods. Copyright © 2007 John Wiley & Sons, Ltd.

INTRODUCTION

The design and control of water infrastructures and systems require the use of design rainfall models to evaluate the effects of intense precipitation events over a certain basin or urban area under study. Despite the reproduction of observed events in natural or urban contexts being carried out within different simulation approaches, the prevailing practice is to generate synthetic hyetographs consistent with the intensity–duration–frequency (IDF) curve that corresponds to the desired return period. Assuming uniformly distributed precipitation in space, as is common over relatively small basins, the duration and the form of the hyetograph are thus to be defined. Parameters governing the form of the resulting precipitation pattern are to be determined so as to optimize flood discharge estimates.

The analysis of the literature concerning the issue of design hyetographs suggests that the rectangular form proposed in the rational method (e.g. Pilgrim and Cordery, 1993) is the most widespread, probably due to its simplicity of use. Several similar formulations were derived after the introduction of the rational method, aimed at providing better estimates of the flood discharge. Some examples are the variational method (e.g. Fiorentino *et al.*, 1987) and the approach proposed by Hua *et al.* (2003). More complex hyetograph shapes have been proposed, such as the triangular hyetograph (Yen and Chow, 1980), the Sifalda hyetograph (Sifalda, 1973), the Desbordes hyetograph (Desbordes and Raus, 1980), the Chicago hyetograph (Keifer and Chu, 1957), and the best linear unbiased estimation (BLUE) hyetograph (Veneziano and Villani, 1999). Recently, Grimaldi and Serinaldi (2006) developed a multivariate approach to define design rainfall patterns in a probabilistic way, and Lin *et al.* (2005) proposed a procedure to evaluate design hyetographs at ungauged sites.

Such a wide variety of design hyetograph shapes often creates confusion about which procedure should be adopted in research and design practice in order to obtain correct flood peak estimates. The goal of this paper is to overcome these issues by analysing five different hyetographs in order to assess their relative performance while predicting flood peak discharges and to evaluate whether specific variations in the parameters involved in the process can influence the results of their application.

The next section describes the simulation strategy, together with the methods adopted to generate the rainfall time-series, the design hyetographs, and the basin unit hydrograph (UH). The third section discusses the simulation results, starting from an initial set of conditions; then the procedure is applied to a wide range of basin

---
* Correspondence to: Lorenzo Alfieri, Lorenzo Alfieri, Dipartimento di Idraulica, Trasporti ed Infrastrutture Civili, Politecnico di Torino, Corso Duca degli Abruzzi 24, 10129 Turin, Italy.
E-mail: lorenzo.alfieri@polito.it

characteristics and rainfall patterns, in order to understand if and how different parameter values affect the results. Some conclusions are drawn in the final section.

DESCRIPTION OF THE SIMULATION STRATEGY

The purpose of this paper is to compare the ability of different design hyetographs to produce consistent estimates (i.e. with the correct frequency of occurrence) of design floods: in the ideal conditions of linearity and stationarity of the rainfall–runoff transformation, one would expect that a design hyetograph characterized by a return period of T years would produce a discharge with the same return period.

Performances are compared within a simulation framework, built on the following points:

1. An ideal river basin with a linear and time-invariant hydrologic response is defined, and its UH, with a specific time step, is derived accordingly (see 'Basin and unit hydrograph description' section).
2. A synthetic time-series of effective rainfall is generated using the iterated random pulse (IRP) model (Veneziano and Iacobellis, 2002) (see 'Rainfall generation model' section). Effective rainfall is defined as the fraction of precipitation that reaches the basin outlet as surface flow. In what follows, for simplicity, we will refer to it as rainfall.
3. The continuous rainfall record is routed through the UH, obtaining the corresponding streamflow timeseries. The series of annual maxima is then extracted from the continuous rainfall record, and the 'real' design discharge $Q(T)$ is selected.
4. The parameters of the IDF curves are estimated from the same synthetic rainfall record, and the five different T-year design hyetographs stem from these curves (see 'Design hyetographs' section). Since the hyetographs are to be convolved with the UH, they have to be resampled with the same time step Δt of the UH. We set $\Delta t = 15$ min, which corresponds to the time step of the continuous rainfall series.
5. The five design hyetographs are convolved with the UH, obtaining a set of design hydrographs, whose maxima $Q_D(T)$ are taken as the estimates of the T-year flood discharges.
6. The estimated and 'real' T-year floods can finally be compared. If we define the variable

$$E_Q = \frac{Q_D(T) - Q(T)}{Q(T)} \times 100 \qquad (1)$$

as the percentage error between estimated and 'real' peak flow, then we can state that the lower the absolute value of E_Q is, the better the accuracy of a design hyetograph is.

Although the proposed method could allow one to assess the whole shape of the output flood hydrographs,

the present work is focused solely on the evaluation of the peak discharge.

Basin and unit hydrograph description

We take under consideration an 'ideal' river basin, with a linear and time-invariant hydrologic response. The rainfall–runoff transformation process is thus identified by simply defining (i) the temporal sequence of excess precipitation $I(t - \tau)$, and (ii) a response function $u(\tau)$ in the form of an instantaneous UH (IUH).

The IUH theory provides an estimation of the discharges $q(t)$ by means of the convolution integral:

$$q(t) = \int_0^t I(t - \tau)u(\tau)\, d\tau \qquad (2)$$

Since the basin is fictitious, we can arbitrarily impose the shape of its IUH to make it suitable for our simulation purposes. We represent the IUH through a three-parameter Beta distribution, whose flexibility allows one to reproduce a wide range of realistic shapes, as shown by Bhunya *et al.* (2004). Differently from other commonly used IUH shapes (e.g. Gamma distribution, Weibull, etc.) the Beta distribution has a finite duration. This is an important property, since the extent of the distribution can be set equal to the concentration time of the basin, avoiding conceptual and numerical problems arising for the slowly decaying tails of the other above-mentioned functions.

The probability density function (PDF) of the Beta distribution is (e.g. Johnson *et al.*, 1995; Kottegoda and Rosso, 1998)

$$p_X(x) = \frac{1}{B(p_\beta, q_\beta)} \frac{(x - a_\beta)^{p_\beta - 1}(b_\beta - x)^{q_\beta - 1}}{(b_\beta - a_\beta)^{p_\beta + q_\beta - 1}}$$
$$a_\beta \leq x \leq b_\beta \qquad (3)$$

where a_β and b_β are the boundary values for x, p_β and q_β are parameters, and

$$B(p_\beta, q_\beta) = \int_0^1 x^{p_\beta - 1}(1 - x)^{q_\beta - 1} dx = \frac{\Gamma(p_\beta)\Gamma(q_\beta)}{\Gamma(p_\beta + q_\beta)} \qquad (4)$$

is the Beta function ($\Gamma(\cdot)$ represents the Gamma function).

When Equation (3) is used to represent the IUH, a_β is set to zero and b_β corresponds to the concentration time of the basin ($b_\beta = t_C$). Hence, a Beta distribution-shaped IUH has the form

$$u(t) = \frac{1}{B(p_\beta, q_\beta)} \frac{t^{p_\beta - 1}(t_C - t)^{q_\beta - 1}}{t_C^{p_\beta + q_\beta - 1}} \qquad (5)$$

Actually, it is preferable to write Equation (5) as a function of parameters with a clearer physical meaning, such as the first two moments of the distribution. The mean of the Beta IUH is

$$E(t) = t_C \frac{p_\beta}{p_\beta + q_\beta} = t_L \qquad (6)$$

where t_L is the lag time of the basin. The variance of the IUH is

$$\sigma^2(t) = t_C^2 \frac{p_\beta q_\beta}{(p_\beta + q_\beta)^2 (p_\beta + q_\beta + 1)} \qquad (7)$$

Parameters p_β and q_β of Equation (5) are then linked to t_L and $\sigma^2(t)$ as follows:

$$p_\beta = \frac{t_L^2}{\sigma^2(t)} \left(1 - \frac{t_L}{t_C}\right) - \frac{t_L}{t_C} \qquad (8)$$

$$q_\beta = p_\beta \left(\frac{t_C}{t_L} - 1\right) \qquad (9)$$

Finally, the corresponding discrete UH is derived by resampling the continuous IUH with the same time step as that of the precipitation time series (15 min).

Rainfall generation model

The IRP model (Veneziano and Iacobellis, 2002) is adopted to generate rainfall time-series. The IRP is a pulse-based representation of temporal rainfall with multifractal properties in the small-scale limit.

The model has six parameters, which allow one to control a wide range of rainfall statistics such as the spectrum, the duration of wet and dry periods, the distribution of rainfall intensities for different aggregation periods, the moment-scaling function, etc.

In the rainfall representation, the IRP model distinguishes between an exterior and an interior submodel. The exterior model is a coarse representation of precipitation events; it is characterized by four groups of 12 monthly-scale parameters: the mean value m_I of the average rainfall intensity during the synoptic events, the mean duration of the wet periods $m_{\tau\,wet}$, the mean duration of the dry periods $m_{\tau\,dry}$, and the exponent k of the Weibull distribution of the dry periods. The purposes of the present work do not include a seasonality analysis; as a consequence, a constant value for each of the four groups of parameters is used for all months.

The interior model describes the fluctuations of rainfall intensity at subsynoptic scales. Precipitation is represented as the superposition of pulses with a hierarchically nested structure of temporal occurrences and a cascade-like dependence of the intensities. Two parameters have to be defined in the interior model: the multiplicity r of the discrete cascade and the so-called co-dimension C_1, which controls the multifractal properties of rainfall at small scales (see Veneziano and Iacobellis (2002) and Veneziano *et al.* (2002)).

Once the six parameters are set, the IRP model provides a synthetic rainfall time-series over a specified number of years (1000 years in the present work) with a 15 min time step.

An analytical IDF curve can then be obtained from this record, analysing the annual maxima of the rainfall intensities for different durations. A three-parameter representation is chosen here:

$$i(d, T) = \frac{a(T)}{(b(T) + d)^{c(T)}} \qquad (10)$$

where $i(d, T)$ is the rainfall intensity corresponding to a duration of d hours and to a return period of T years. The three parameters $a(T)$, $b(T)$ and $c(T)$ are estimated by fitting the IDF function to the empirical values using a non-linear least-squares method. The procedure comprises the following steps: the annual maxima are extracted from the synthetic rainfall record for durations ranging from 15 min to 24 h. For each duration, the vectors of the n maxima are sorted in ascending order and an empirical return period T is associated to the jth value in this ordered series, with

$$\frac{j}{n+1} = 1 - \frac{1}{T} \qquad (11)$$

Two kinds of IDF curve are then calculated. The first is obtained by fitting Equation (10) to the mean values of the 1000 annual maxima of the rainfall intensities, one for each duration considered. The resulting IDF curve, $\bar{i}(d) = \bar{a}/(\bar{b} + d)^{\bar{c}}$, is henceforward referred to as $\overline{\text{IDF}}$. The second kind is a family of IDF curves, found by fitting Equation (10) to the annual maxima characterized by the same empirical return period. The resulting curves are henceforward referred to as IDF(T). Figure 1 shows some examples of IDF(T) for different return periods, together with the $\overline{\text{IDF}}$ and the empirical points available for the durations considered. In particular, Figure 1 shows cumulated precipitation depths h rather than intensities: $h(d, T) = i(d, T)d$. It can be noted that the three-parameter representation (Equation (10)) provides a very good fit to the empirical data.

Design hyetographs

In this section we describe the five hyetograph formulations we have considered, which were chosen because of their widespread practical use. Other approaches that are available in the literature were not examined because they are less commonly used or represent modifications of these five formulations (e.g. the Sifalda hyetograph).
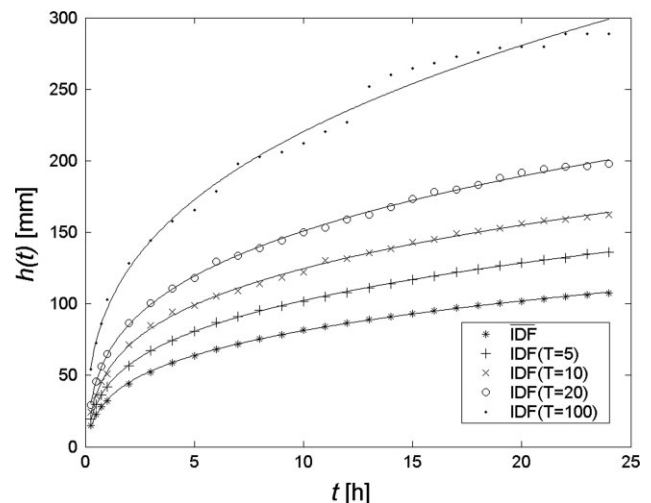
Figure 1. IDF curves for different return periods: empirical points and analytical curves from Equation (10)

1. The first one consists of a constant rainfall intensity over a time span equal to the concentration time of the basin t_C. This formulation is consistent with the use of the rational method to produce estimates of the design flood (e.g. Pilgrim and Cordery, 1993) and it is henceforward referred to as Rational (t_C). The precipitation intensity value is obtained from the IDF curve, $i(t_C, T)$, with the desired return period.

2. The second design hyetograph is analogous to the first, except that the rainfall duration is set equal to the basin lag time t_L (e.g. Fiorentino *et al.*, 1987). Again, the constant rainfall intensity, $i(t_L, T)$, is obtained from the IDF curve for a given return period. This method is hereinafter referred to as Rational (t_L).

3. The variational method also produces a rectangular design hyetograph, characterized by a couple of values, intensity i^* and duration t^*, again taken from a point on the IDF curve. In this case, a couple of values are chosen to maximize the resulting peak outflow (see Fiorentino *et al.* (1987)). Practically, this method selects the constant-intensity hyetograph, among all those compatible with the IDF curve, which generates the highest peak discharge when convolved with the corresponding basin UH. It follows that the characteristics of such a hyetograph (i.e. intensity i^* and duration t^*) will be affected by the parameters of the IDF curve and by those of the UH as well.

A simple generalized form can be defined, which holds for the three design hyetographs described above:

$$I(t, T) = i(t', T) \quad 0 \leq t \leq t'$$
$$I(t, T) = 0 \qquad\qquad t > t' \tag{12}$$

where $t' = t_C$ for the Rational (t_C), $t' = t_L$ for the Rational (t_L), and $t' = t^*$ for the Variational method.

4. The Chicago hyetograph (Keifer and Chu, 1957) is defined so that for each duration the precipitation intensity is congruent with the IDF curve. In contrast, in the three previous cases, the precipitation depths match the IDF only for durations equal to the total length of the hyetograph. With the assumed three-parameter IDF curve (Equation (10)) and defining $r_C = t_r/t_C$ as the ratio between the peak position t_r and the concentration time t_C, we obtain the following formulation of the Chicago hyetograph:

$$I(t, T) = a(T) \frac{b(T) + (1 - c(T))\dfrac{t_r - t}{r_C}}{\left(b(T) + \dfrac{t_r - t}{r_C}\right)^{c(T)+1}} \qquad \text{for } t \leq t_r \tag{13}$$

and

$$I(t, T) = a(T) \frac{b(T) + (1 - c(T))\dfrac{t - t_r}{1 - r_C}}{\left(b(T) + \dfrac{t - t_r}{1 - r_C}\right)^{c(T)+1}} \qquad \text{for } t \geq t_r \tag{14}$$

In this study, the peak position of the Chicago hyetograph is always set to the midpoint, i.e. $r_C = 0.5$.

Some considerations are reported in the concluding remarks concerning the influence of such a choice on the results.

5. The BLUE hyetograph (Veneziano and Villani, 1999) aims at estimating the most likely sequence of rainfall intensities $I(t_C - t)$ associated with a given peak discharge $Q(T)$, by means of the BLUE theory (e.g. Sorensen, 1980: chapter 4). The BLUE hyetograph depends explicitly on the correlation characteristics of the rainfall process and on the basin IUH.

The general expression for $I(t_C - t)$, i.e.

$$I(t_C - t, T) = m_y + \frac{Q(T) - m_q}{\sigma_q^2} \int_0^\infty B_y(t - \tau)u(\tau)\, d\tau \tag{15}$$

is a function of the mean value m_y and of the covariance function B_y of the rainfall process, of the peak discharge $Q(T)$, of the mean value m_q and the variance σ_q^2 of the flow q, and of the shape of the IUH $u(\tau)$.

Two simplified formulations have been proposed for Equation (15) for particular values of the ratio $\eta = \tau_0/t_L$ between the autocorrelation of the rainfall intensities and the lag time of the basin. In particular, τ_0 represents the time lag that satisfies the relation $\rho(\tau_0) = 1/e$, where ρ is the rainfall autocorrelation function, $\rho = B_y/\sigma_y^2$, and e is the Euler number. When $\eta > 20{-}30$, i.e. for a narrow IUH compared with the correlation time of the rainfall process, the design hyetograph approaches a shape that is the mirror image of the rainfall correlation function. On the other hand, when $\eta < 0.5{-}0.7$, i.e. for a wide IUH or weakly correlated rainfall, Equation (15) can be simplified to

$$I(t_C - t, T) = Q(T) \frac{u(t)}{\displaystyle\int_0^\infty u^2(\tau)d\tau} \propto u(t) \tag{16}$$

In Equation (16) the design hyetograph is proportional to the mirror image of the IUH (since the sequence of rainfall intensities is expressed as a function of a negative time). The condition $\eta < 0.5{-}0.7$ is often met for rather large or medium-scale basins, since τ_0 is usually of the order of 1 h or less (Veneziano and Villani, 1999).

In our applications, the peak discharge $Q(T)$ is an unknown quantity; hence, it is assumed that the total amount of rainfall carried by the BLUE hyetograph is congruent with the IDF curve with a given return period. Since the duration of the hyetograph is t_C, the coefficient $Q(T)/\int_0^\infty u^2(\tau)\, d\tau$ from Equation (16) is set equal to $h(t_C, T)$. This leads to the final form of the hyetograph:

$$I(t_C - t, T) = h(t_C, T)u(t) \tag{17}$$

It is further worth noting that the BLUE hyetograph is the only of the five that can produce rainfall intensities that exceed the IDF curve. In fact, the distribution of the rainfall intensities within the hyetograph is constrained only by the shape of the IUH of the basin.

The five design hyetographs considered are shown in Figure 2. Note that the total amount of rainfall carried by the Rational (t_C), Chicago and BLUE hyetographs is the same, but the rainfall patterns are very different, with peak intensities varying between 8 and 56 mm h^{-1}. The rainfall volumes associated with the Rational (t_L) and the variational method are, instead, lower, in that they are characterized by rainfall events with lower durations and higher intensities compared with the Rational (t_C), though they stem from the same IDF curve.

RESULTS AND DISCUSSION

Reference case

We first focus on a reference case with an initial set of rainfall characteristics and UH parameters. Initial IRP parameters are hereby set, following Veneziano and Iacobellis (2002), as: $m_{\tau \, wet} = 25$ h, $m_{\tau \, dry} = 100$ h, $k = 0.44$, $m = 0.15$ mm/15 min for the exterior model; $r = 4$, $C_1 = 0.1$ for the interior model. Such parameters are typical of midlatitude rainfall regimes and they correspond to a mean annual precipitation depth roughly equal to 1000 mm. We make the assumptions that the time-series generated represents excess precipitation data and that the rainfall depth values are spatially uniform over the basin area.

The characteristics of the Beta-shaped UH are set as follows: $t_C = 10$ h, $t_L = 4$ h and $\sigma(t) = 2$ h. The resulting UH is then obtained from Equation (6), substituting t_L and $\sigma(t)$ in Equation (8) and Equation (9), giving $p_\beta = 2$ and $q_\beta = 3$ (e.g. see Figure 4a, bold line).

In the reference case we analyse the mean annual flood, i.e. we estimate the five design hyetographs from the mean IDF curve $\overline{IDF}$. The resulting peak flow estimates are then compared with the mean of the 1000 annual maxima.

The results are shown in Figure 3, in which the BLUE method demonstrates a better performance than the others in terms of estimated peak flow. Among the other methods, the three hyetographs with constant rainfall intensity tend to underestimate the peak flow (Rational (t_C) in particular), while an overestimation is obtained from the Chicago hyetograph.

We proceed with a set of experiments to evaluate the design hyetographs' performance following variations of the main parameters involved. The experiments are carried out by varying one variable at a time, keeping the others equal to the values assumed in the reference case. Five changes are proposed, concerning the modification of (i) the basin lag time t_L, (ii) the dispersion parameter of the UH, (iii) the basin concentration time t_C, (iv) the return period T and (v) the ratio $h(24)/h(1)$ (from Equation (10)) that measures a growth index of the IDF curve. Note that the first three experiments relate to changes in the hydrologic response function, whereas the last two concern variations in the climatic model. In the following subsections, each experiment is described in detail and the related results are discussed.

Changes in the basin lag time

Different parameterizations of the Beta function representing the UH are considered, keeping the same concentration time and standard deviation used in the reference case but varying the lag time between $0.2t_C$ and $0.8t_C$ (see Figure 4a).

The application of the procedure described in the 'Description of the simulation strategy' section allows one to represent the results in terms of percentage error E_Q from Equation (1). All of the methods considered provide an almost constant error E_Q for lag times between 3 and 7 h. In more detail, Figure 4b shows an overestimation for the Chicago and BLUE hyetographs (this latter seems to be the method that produces the minimum value for $|E_Q|$) and underestimations, especially for the Rational (t_C) method, produced by the remaining three hyetographs. An interesting result is that the Rational (t_L) method produces results that are, for a wide range
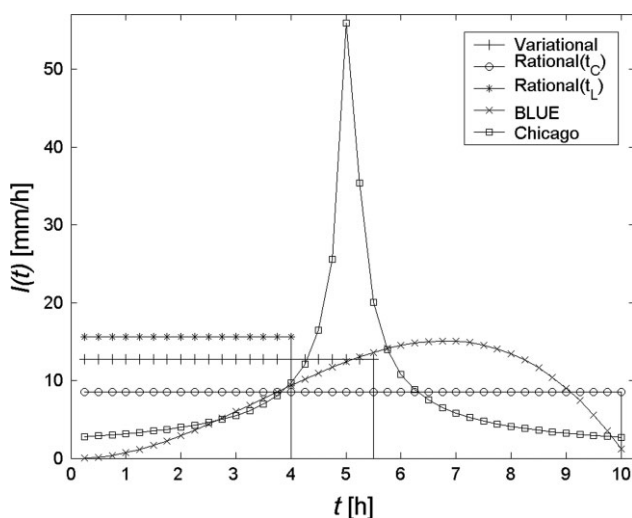
Figure 2. Comparison among the five design hyetographs considered in this paper, with parameters corresponding to the reference case (see 'Reference case' section)
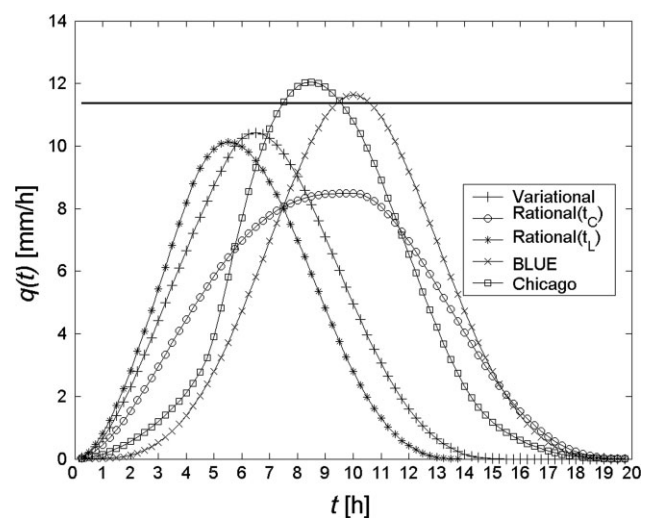
Figure 3. Comparison among the hydrographs obtained for the reference case. The horizontal bold line is the value of $Q(T)$ derived from the flood frequency analysis
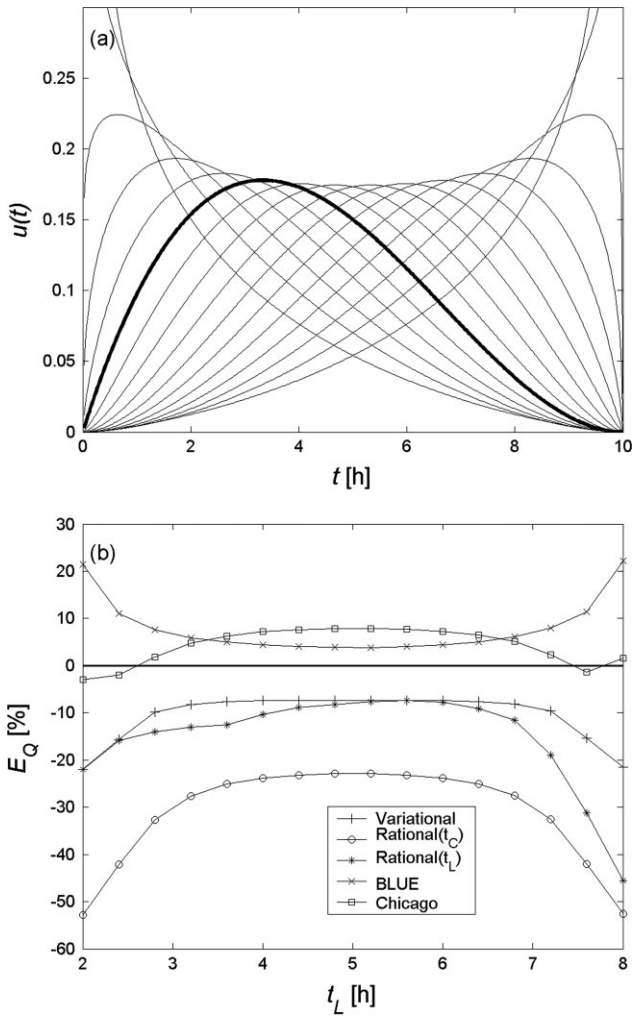
Figure 4. (a) The UH shapes; the bold line is the UH adopted in the reference case. (b) Variability of the relative error E_Q for each design hyetograph as a function of the basin lag time

a lower discharge. On the other hand, the BLUE hyetograph yields strong overestimations, because a 10 h precipitation depth from Equation (10) is distributed over only 6 h, thus generating a hyetograph that exceeds the IDF curve for several durations. However, it should be pointed out that it is unlikely for a basin to have a UH with features similar to those of a Beta curve with such small values of $\sigma(t)$.

Changes in the basin concentration time

Keeping the same shape as in the initial case, the UH is rescaled by a set of different concentration times, ranging between 2·5 and 30 h. The lower limit is mainly constrained by the simplification introduced in the 'Design hyetographs' section for the BLUE hyetograph, which allows one to transform Equation (15) into Equation (16); moreover, the calculation time step is set to 15 min, and smaller values of t_C would produce inaccurate UHs and hyetographs. The results obtained (Figure 6) show an increasing overestimation for the BLUE hyetograph as t_C decreases. Again, the Rational (t_C) method provides large underestimations, which increase with t_C, whereas the responses of the Chicago, variational and Rational (t_L) hyetographs seem to be almost independent of the concentration time.
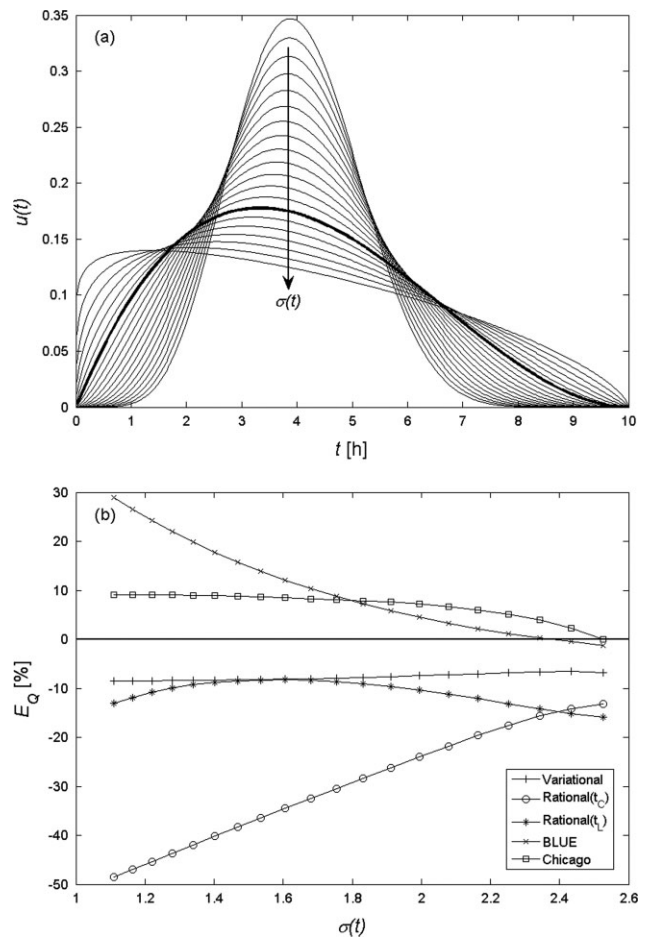
Figure 5. (a) The IUH shapes; the bold line is the UH adopted in the reference case. (b) Variability of the relative error E_Q for each design hyetograph as a function of the standard deviation of the basin UH

of t_L values, very close to those obtained with the more cumbersome variational method.

Changes in the dispersion of the unit hydrograph

In this case we produce a set of Beta UHs with lag time and concentration time as in the reference case, but characterized by a progressive variation of their dispersion (see Figure 5a). From Equations (8) and (9), substituting $t_L = 4$ h and $t_C = 10$ h, we obtain the parameters to adopt in Equation (5) in order to generate UH shapes with different standard deviations. Figure 5b shows a general pattern similar to that of the previous case, the main difference being a deterioration of the results obtained with the Rational (t_C) and the BLUE hyetographs as $\sigma(t)$ decreases, i.e. with very peaky UHs. In fact, for small values of $\sigma(t)$ (e.g. $\sigma(t) = 1\cdot1-1\cdot2$) almost the whole area of the UH is included in about 6 h out of the total 10 h (see Figure 5a); this means that, for the Rational (t_C) method, a rainfall intensity from the IDF curve for a duration of 10 h goes in a convolution integral with a UH just 6 h long, producing, therefore,

Figure 6. Variability of the relative error E_Q for each design hyetograph as a function of the basin concentration time

Changes in the return period of flood discharge

Different IDF curves are obtained from integer values of T ranging between 2 and 100 years (from Equation (10)) to be used in the procedure described in the 'Description of the simulation strategy' section. Each hydrograph peak obtained is then compared with the jth element of the empirical distribution for the same return period (from Equation (11)).

The results, in Figure 7, show irregular fluctuations of the values of E_Q for all of the methods considered that arise from considering T-year peak discharge values obtained from an empirical distribution, characterized by an irregular form compared with the analytical distributions. The E_Q points obtained can be represented quite accurately by linear trends, with very similar slopes. The results, for every return period, show considerable underestimations provided by the methods characterized by a constant precipitation intensity (especially for the Rational (t_C)). Slight overestimations are instead provided by the BLUE and the Chicago hyetographs.
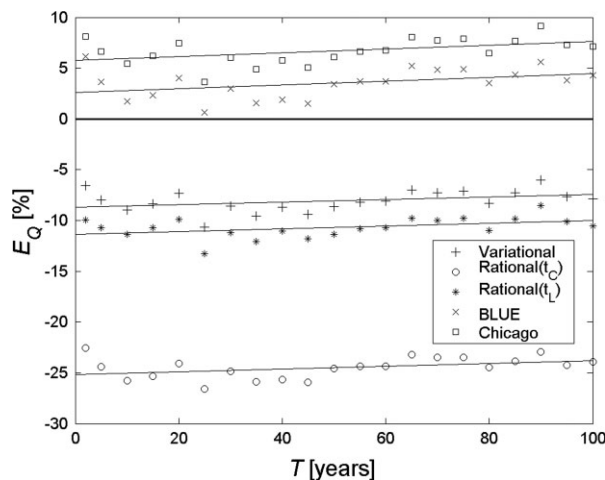
Changes in the shape parameter of the intensity–duration–frequency curve

To examine the impact of changes in the IDF curve, an additional set of 12 excess precipitation time-series has been generated by means of the IRP model. Since the IDF parameters are not explicit input data in the IRP model, we proceeded by trial and error, by adjusting the six IRP parameters to obtain the required changes of the IDF characteristics. We found that consistent results are obtained by keeping five IRP parameters as those of the reference case and varying only the interior model co-dimension C_1 between 0 and 0·3. The resulting IDF curves are summarized by their $h(24)/h(1)$ ratios (i.e. the ratio between the 24 h and the 1 h precipitation depths), which range between 2·3 and 4·6. The results obtained for each design hyetograph are shown in Figure 8. The BLUE hyetograph provides better estimations for a wide range of abscissas, but it is also very variable with the IDF shape parameter $h(24)/h(1)$. Results from the Rational (t_L) method are very close to those of the variational method for low values of the shape parameter, but the outcomes tend to diverge as $h(24)/h(1)$ increases. The Rational (t_C) method always provides large underestimations, which are more evident for low values of the abscissas.

CONCLUDING REMARKS

A simple framework to test some design hyetographs for the evaluation of the peak discharge during flood events is described. A set of simulation experiments has been carried out in order to evaluate the influence of the different variables involved in the testing framework, to emphasize the major advantages and drawbacks of each hyetograph formulation.

On analysing the results obtained in the simulation experiments, some general conclusions arise regarding the five formulations tested. In most cases the

Figure 7. Variability of the relative error E_Q for each design hyetograph as a function of the return period of the peak flow
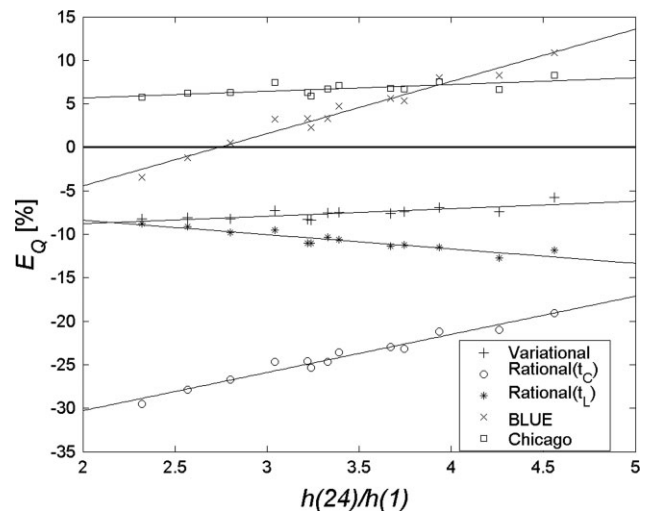
Figure 8. Variability of the relative error E_Q for each design hyetograph as a function of the ratio $h(24)/h(1)$ between the 24 h and the 1 h rainfall depths. Linear trends interpolating the points are also shown

BLUE hyetograph produces better results than the other methods; nevertheless, a strong dependence is observed between the errors E_Q obtained and some of the variables tested, in particular towards the dispersion of the basin UH, the concentration time and the shape parameter of the IDF curve.

The variational method and the two rational methods always provide underestimations of the peak discharge with respect of the values obtained from the flood frequency analysis. Whereas the Rational (t_C) method often appears inaccurate and quite variable with changes in the model parameters, the two other 'rational-derived' formulations frequently provide good results, with an error E_Q around -10%. The adoption of the Rational (t_L) instead of the more complex variational method then results in a reasonable approximation for a wide range of situations. In itself, the variational method presents underestimated results, but with excellent stability with respect to the variability of parameters. Some considerations on the Chicago hyetograph are to be drawn as well: on the one hand, it always provides overestimations of the peak discharge; on the other hand, it is characterized by a very stable bias (E_Q) in all of the five experiments. Therefore, a sensitivity analysis on the Chicago hyetograph was carried out to understand whether the peak position can affect the flood discharge estimates. Our findings can be summarized as follows.

1. The peak position of the Chicago hyetograph does affect peak flow estimation, with E_Q values that range between roughly -10% and $+8\%$, all other parameters being equal.
2. The peak position also plays an important role in the variability of the results provided, especially when changes in the basin lag time and in the dispersion of the UH are considered.
3. The Chicago hyetograph with midpoint peak, as mentioned, always produces overestimations, but it is the most stable in its results. It is then confirmed as the most suitable amongst all the possible variations.

In conclusion, both the variational and the Chicago (with $r_C = 0.5$) hyetographs provide biased estimates, but very stable with respect to basin and climatic parameters, thus allowing one to define correction factors for removing the bias. The correction multiplicative factor we found for the Chicago method is 0·94, and the one related to the variational method is 1·08. Such a procedure allows one to achieve values of $|E_Q|$ that are below 2% for most of the IUH shapes and the climatic parameters.

Of course, these results are strictly valid when the simplifying assumptions we described throughout this paper are maintained (i.e. linearity and time invariance of the response function, known effective rainfall, constant rain rate over the whole basin area). However, such sources of uncertainty affect the five formulations to the same extent and their evaluation is independent of the hyetograph definition. As a consequence, the results mentioned are also valuable for real-world applications, in particular in that they show how some design hyetographs commonly adopted in engineering practice (e.g. Rational (t_C)) provide poor performance in the evaluation of the peak flood discharge.

REFERENCES

Bhunya PK, Mishra SK, Ojia CSP, Berndtsson R. 2004. Parameter estimation of Beta distribution for unit hydrograph derivation. *Journal of Hydrologic Engineering* **9**: 325–332.

Desbordes M, Raous P. 1980. Fondaments de l'élaboration d'une pluie de projet urbaine. Méthodes d'analyse et application à la station Montpellier Bel Air. *La Météorologie, VI série* **20–21**: 317–326.

Fiorentino M, Rossi F, Villani P. 1987. Effect of the basin geomorpho-climatic characteristics on the mean annual flood reduction curve. In *Modeling & Simulation Vol. 18: Proceedings of the 18th Annual Pittsburgh Conference on Modeling and Simulation*, Part 5. International Society for Measurement and Control; 1777–1784.

Grimaldi S, Serinaldi F. 2006. Design hyetographs analysis with 3-copula function. *Hydrological Sciences–Journal-des Sciences Hydrologiques* **51**: 223–238.

Hua J, Liang Z, Yu Z. 2003. A modified rational formula for flood design in small basins. *Journal of the American Water Resources Association* **39**: 1017–1025.

Johnson NL, Kotz S, Balakrishan N. 1995. *Continuous Univariate Distributions*, volume 2. Wiley.

Keifer CJ, Chu HH. 1957. Synthetic storm pattern for drainage design. *ASCE Journal of the Hydraulics Division* **83**(HY4): 1–25.

Kottegoda NT, Rosso R. 1998. *Statistics, Probability and Reliability for Civil and Environmental Engineers*. McGraw-Hill: New York; 212–214.

Lin GF, Chen LH, Kao SC. 2005. Development of regional design hyetographs. *Hydrological Processes* **19**: 937–946. DOI: 10·1002/hyp.5550.

Pilgrim DH, Cordery I. 1993. Flood runoff. In *Handbook of Hydrology*, vol. 9, Maidment DR (ed.). McGraw-Hill: New York; 1–42.

Sifalda V. 1973. Entwicklung eines Berechnungsregens für die Bemessung von Kanalnetzen. *GWF-Wasser/Abwasser* **114**: 435–440.

Sorensen HW. 1980. *Parameter Estimation*. Marcel Dekker: New York.

Veneziano D, Iacobellis V. 2002. Multiscaling pulse representation of temporal rainfall. *Water Resources Research* **38**: 1138. DOI: 10·1029/2001WR000522.

Veneziano D, Villani P. 1999. Best linear unbiased design hyetograph. *Water Resources Research* **35**: 2725–2738.

Veneziano D, Furcolo P, Iacobellis V. 2002. Multifractality of iterated pulse processes with pulse amplitudes generated by a random cascade. *Fractals-Complex Geometry Patterns and Scaling in Nature and Society* **10**: 209–222.

Yen BC, Chow CT. 1980. Design hyetographs for small drainage structures. *Journal of the Hydraulics Division* **106**: 1055–1076.